Networking Experiments in the Keio Future Photonic Network Open Laboratory with Field-installed Hollow-Core Optical Fiber Cables

Satoru Okamoto
Keio Frontier Research & Education Collaborative Square at Shin-Kawasaki
Keio University
Kawasaki-shi, Kanagawa, Japan
https://orcid.org/0000-0002-4742-261X

***Abstract*—The Keio Future Photonic Network Open Laboratory was opened in Apr. 2023 as a testing field for future Beyond 5G networking technology. This paper presents a proof-of-concept system for the new multi-access edge computing technology "AMec" using OpenLab's networking equipment, and actual application verification experiments using newly installed Hollow-Core optical fiber cables at OpenLab.**

Keywords—beyond 5G, low latency, multi-access edge computing, hollow-core fiber, passive optical network, private 5G

I. INTRODUCTION

Optical network technologies and its networking technologies have made great progress in terms of high-speed, large capacity, and dynamic link technology, and computer science services such as cloud services have also been enhanced. In the Beyond 5G (B5G) era, specifically encourages further development in seven areas (ultra-fast and large capacity, ultra-low latency, ultra numerous connectivity, ultra-low power consumption, ultra security and resiliency, autonomy, and scalability) [1, 2], with ultra-low latency and ultra-low power consumption among the top priorities. Ultra-low latency services are in high demand for new smart social services such as robot control and autonomous driving vehicle (ADV). In addition, ultra-low latency is important not only in the conventional wireless access section (several 100 m to 1 km area) but also in a certain range (we call it as "area space" which is approximately 10 to 20 km area). On the other hand, ultra-low power consumption is also a goal of the sustainable development goals (SDGs), and there are high expectations for photonics device technology, which can achieve power savings of up to 1/1,000 compared to current electricity.

The Keio Future Photonic Network Open Laboratory (OpenLab) is a testing field of the Keio Future Optical Network Open Research Center focusing the future B5G networking technologies which cover from a new optical fiber, innovative optical/wireless access systems, to applications on the innovative optical network systems such as multiaccess edge computing (MEC), area space computing, and network controlled ADVs. This article describes networking experiments conducted by Keio University's "Keio Future Photonic Network Open Laboratory".

This work is partly supported by the R&D of innovative optical network technologies for a green society project (JMPI00316) funded by the Ministry of Internal Affairs and Communications Japan and JGN (TB-A22001).

II. KEIO FUTURE PHOTONIC NETWORK OPEN LABORATORY

A. Keio Future Optical Network Open Research Center

Fig. 1 shows the targets of B5G compiled by the Ministry of Internal Affairs and Communications (MIC)'s B5G Wired Network Study Group in Japan. They set out to achieve a major breakthrough in ultra-low power and ultra-low latency using optical network technologies and photonics devices. In order to achieve ultra-low latency, a breakthrough from not only protocol level but also the device level is essential. And at the same time, we would like to aim for a paradigm shift that vertically integrates networks, systems, and even their applications. In that case, a system that collaborates with researchers and engineers, including many application researchers, is essential. To establish this feature, the Keio Future Optical Network Open Research Center [3] was created in April 2023 with support from the MIC of Japan.

Fig. 2 show a structure of the Keio Future Optical Network Open Research Cetner. The Keio Future Photonic Network Open Laboratory is a main activity of this research center and affiliated with other open laboratories such as OpNeAR (Open Networking Advanced Research Lab.) in UTD [4] and Keihanna Open Lab. [5]. The Keio Future Optical network Open Research Center has been installed the hollow-core fiber (HCF) cables (describes in *C*) [6] on its campus to achieve ultra-low latency not only on the rack or in the floor but also on the multi-building campus. The OpenLab can be used by researchers from domestic and international companies and universities by sharing their research objectives.

B. Networking Equipment of the Keio Future Photonic Network Open Laboratory

The OpenLab has the small server clusters (mini-data centers (DCs)) for both MEC environment (MEC-DC) and cloud environment (cloud-DC). These DCs are connected using the JGN's [7] Ethernet service. The JGN connects the Keio-Shina-Kawasaki (K2) campus of the Keio University in Kanagawa Prefecture, Japan and Koganei Keihanna Open Lab. at National Institute of Information and Communications Technology (NICT) in Tokyo Metropolitan area, Japan. Physically the

979-8-3503-8461-1/24/$31.00 ©2024 IEEE

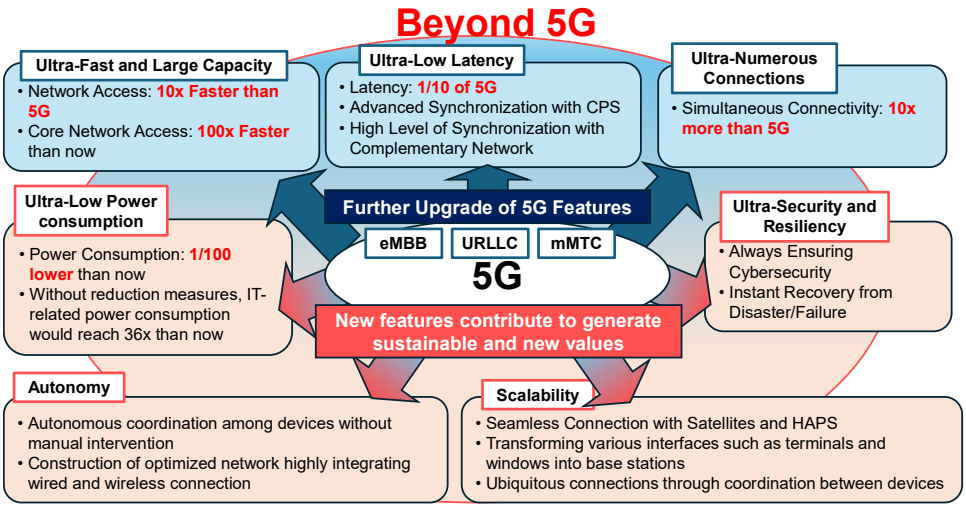

Fig.1 Kye Features for Beyond 5G.

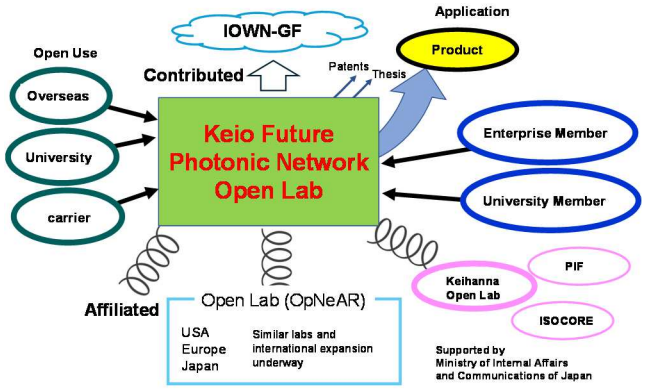

Fig.2 A structure of the Keio Future Optical Network Open Research Center.

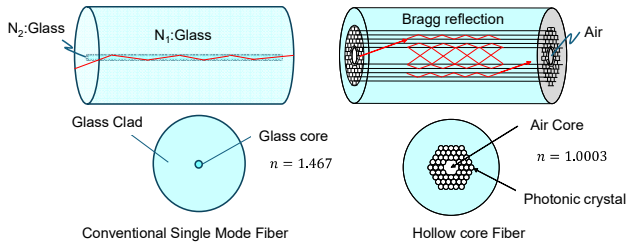

Fig.3 Image of optical transmission using hollow core fiber.

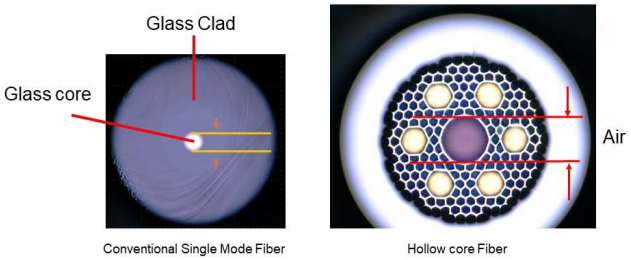

Fig.4 Cross-sectional view of hollow core fiber (Image: size adjusted).

cloud-DC is located in the K2 campus but the round trip time (RTT) between the MEC-DC and the cloud-DC is about 20 ms.

The MEC-DC is connected to two types of access networks. One is a commercial 10 gigabit Ethernet passive optical network (10G-EPON), another is a private 5th generation (P5G) wireless access network. P5G is also called local 5G (L5G) in Japan.

The 10G-EPON is constructed by an optical line terminal (OLT) and optical network units (ONUs). 5 km and 10 km standard single mode fibers (SMFs) are inserted between the OLT and ONUs. As an optical distribution network (ODN), maximum distance of 15 km is set from the ONU to the OLT.

C. Installed Hollow-core Fiber cables

Fig. 3 shows the structures of an ordinary SMF and an HCF. Fig. 4 shows a cross-sectional photograph of the SMF and HCF [6]. This HCF is classified into the photonic bandgap type fiber (PBGF) [8-10]. There is another structure called anti-resonant type HCF [11-13] but because of better performance for practical use, we have installed the PBGF type HCF into the Keio Shin-Kawasaki K2 campus. As shown in Fig. 4, HCFs have a crystal structure in their cladding, and the diameter of the core portion, where light is successfully confined in the air portion of the core through Bragg reflection, is larger than that of SMFs. Since the core is air and refractive index of air is very small (n = 1.000292), the following three major characteristics are expected.

(1) High energy transmission is possible: approximately 1,000 times that of normal glass core optical fiber.

(2) Low latency: $v = C_0/n_{\_HCF}$ and $n_{\_HCF}$ =1.000292 (C_0 is the speed of light: 2.99792458×10^8 m/s), normal glass ore optical fiber's $n_{\_SMF}$ = 1.467. Table 1 shows a theoretical latency differences between SMF and HCF. There are some demonstration related to low latency [10,14-16] this is one of the very important characteristics for B5G.

(3) High linearity: no nonlinearity depending on the core material. This characteristic is new future for optical transmission [17].

From (1), there is a possibility of realizing power over fiber (PWoF) [18] and ultra-multi-wavelength transmission because there is a low limit on energy density increasing in proportion to the number of wavelengths. In (2), there is a possibility of a low-latency network. And by (3), there is a possibility of analog radio over fiber (ARoF) transmission [19]. In this paper, we will report of the experimental result of (2).

TABLE I. LATENCY OF SMF AND HCF FIBERS

Length (m)	SMF latency (μs)	HCF latency (μs)	Latency differences (μs) (SMF-HCF)
300	1.47	1.00	0.47
500	2.45	1.67	0.78
1,000	4.89	3.34	1.56
10,000	48.93	33.37	15.57

III. NETWORKING EXPERIMENTS IN THE KEIO FUTURE PHOTONIC NETWORK OPEN LABORATORY

In this section we will provide two experimental result in the OpenLab. One is a MEC related networking experiment, another is an application over installed HCF experiment.

A. Accenn/Metro Edge Computing (AMec) experiment

Edge computing demand is increasing due to the need for rapid response times and substantial local device resources for numerous applications in B5G era [1]. Additionally, the volume of data transmitted to the cloud is rapidly expanding. Furthermore, modern network devices are now equipped with multi-core processors and are increasingly adopting open, becoming white-boxed [20]. As a result, network devices capable of executing user programs with their surplus resources, which were originally designated for tasks such as data collection and routing reconfigurations, are gaining popularity. We have proposed the access/metro edge computing (AMec) concept [21-24], an innovative edge computing model that leverages underutilized computational resources in network devices, such as central processing units (CPUs) and graphic processing units (GPUs). As shown in Fig. 5, AMec aims to utilize computational resources primarily from network infrastructure components like OLTs, IP routers, Ethernet switches, optical cross-connect systems (OXCs), and reconfigurable optical add/drop multiplexers (ROADMs), which are typically owned by telecom service providers. Therefore AMec service will provided by telecom service providers for enhancing their MEC services.

Traditional MEC systems necessitate the establishment of dedicated servers at edge locations. In comparison, AMec proposes leveraging computational capacities of network devices belonging to service providers, as depicted in Fig. 5. Future plans include the possibility of utilizing idle gaming consoles with GPUs and Internet of Things (IoT) devices in households. AMec's utilization of these resources is intended to accomplish the following goals.

- To process third-party applications offloaded from user equipment or disseminated from cloud platforms.

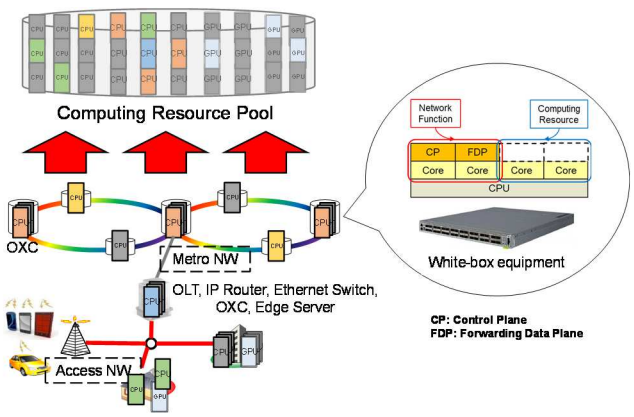

Fig.5 Image of resource pool consisting of xPU on heterogeneous devices.

- To exploit intermittently available computing resources like CPUs in network devices.
- To allocate the most suitable edge resources, taking into account the current availability of resources, user requirements, and the specific needs of applications.

We have designed the sample AMec implementation architecture as illustrated in Fig. 6 [24]. For implementation, we have established clusters using Kubernetes (k8s). Our current plan is to set up a cluster in each prefecture, incorporating network devices and edge servers located in service provider's facilities. AMec services can be offered directly by the service provider or through third parties utilizing the service provider's network equipment for computing. The AMec controller has capabilities beyond what a cluster's master alone can provide, such as intricate pod allocation. The frontend acts as the interface for users. Typically, users only engage with this frontend and remain unaware of the exact location where their tasks are offloaded. Owing to the container-based nature of the system, third-party containers from Docker Hub can be imported and executed within AMec. We have confirmed that application pods are functional on a P4 white-box switch [22].

The detailed pod allocation algorithm and allocation procedure are described in [23] and [24]. In this paper, we will present brief working flow. AMec users only interact with a frontend. The frontend takes an offloading request from a user, and then the AMec controller decides which nodes should process the pods within the applications, instructing the master

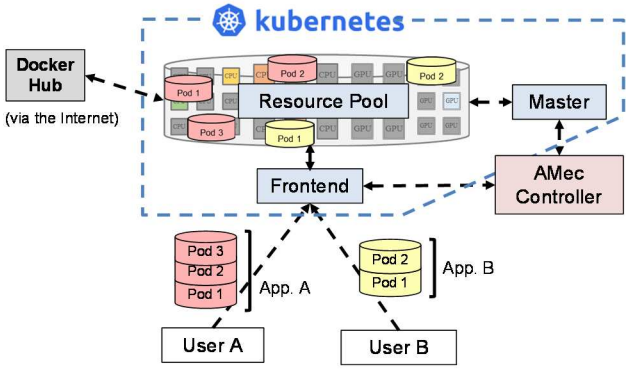

Fig.6 An example of the designed AMec system architecture.

to deploy pods to these nodes. Once the pods are active, the user offloads their processing tasks to the cluster, i.e. resource pool, through the frontend. For determining the appropriate nodes for pod processing within the applications, the AMec controller collects information on each cluster node.

We have created an AMec proof of concept (PoC) system and conducted experiments on it. The purpose of the experiments are the following two points.

- Verification of feasibility: Verify the feasibility of a series of processes from receiving requests from users to running applications on AMec. Especially, the connectivity between the AMec Controller and the k8s system is important and needed to be verify.
- Measure "user waiting times": It is the time between when a user makes a request and when the application starts. We need to measure and analyze the total time and its breakdown.

The architecture of the constructed AMec PoC system is shown in Fig. 7. The AMec PoC system is constructed on three logical regions: the cloud region and two MEC regions. The cloud region is constructed on the OpenStack system located in the OpenLab at Keio-Shin-Kawasaki (K2) campus using the cloud-DC of the OpenLab. One MEC region is constructed on another OpenStack system located in the Keio K2 campus, i.e. the MEC-DC of the OpenLab. Another MEC region is constructed in the Keio Yagami Campus. Both campuses are connected via 1 Gbps dedicated Ethernet line service. The nodes consisting the AMec PoC system is shown in Table 2.

TABLE II. NODE SPECS OF THE CONSTRUCTED AMEC POC SYSTEM

Region	Roll	Equipment	CPU Cores	RAM
OpenStack DC@Keio-K2	AMec Controller	OpenStack Instance	4 (amd64)	8 GB
	k8s-master	OpenStack Instance	4 (amd64)	8 GB
OpenStack MEC@Keio-K2	Frontend	OpenStack Instance	2 (amd64)	4 GB
	k8s-worker	OpenStack Instance	2 (amd64)	4 GB
Keio-Yagami	k8s-worker	Raspberry Pi4	4 (arm)	4 GB
	k8s-worker	Edgecore Wedge P4	16 (amd64)	48 GB
	k8s-worker	Dell R630	4 (amd64)	96 GB

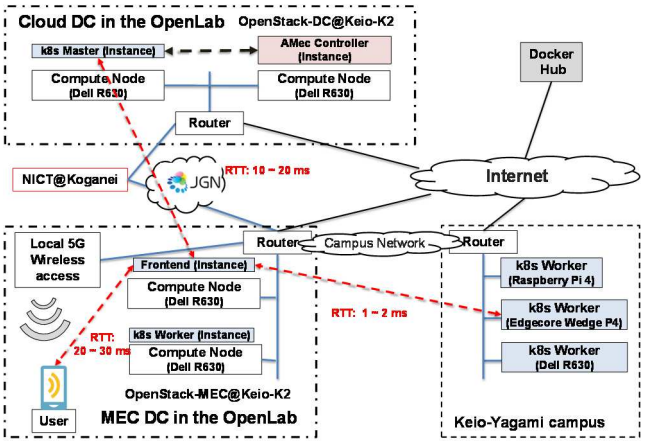

Fig.7 Architecture of the constructed AMec PoC.

Application is run on pods in k8s-workers. Heterogeneous works are provided by server, P4 switch (Edgecore Wedge), and IoT device (Raspberry Pi4). K8s-worker nodes are located in Keio-Yagami and OpenStack-MEC@Keio-K2, while k8s-master and AMec Controller are located in OpenStack-DC@Keio-K2. Both OpenStack-MEC and OpenStack-DC are located in the same room of the OpenLab (Fig. 8), but they are connected via JGN [7] with a turnaround at NICT in Koganei. Therefore, there is a large latency between k8s-master and the instance rolled Frontend. The RTT is almost 20 ms.

A user accesses the frontend via a Local 5G (L5G) wireless access network. The base station of the L5G system is run on the commodity type server system (Fig.9). Therefore, RTT from user terminal to the frontend was over 20 ms. The user sends a request to the frontend saying that it wants to start an application. In this experiment, we assumed that the application requires three pods. Each pod requires CPU resource of 0.5, 1.0, and 1.5 vCPU, respectively. Average run time of this application is 5 minutes. For evaluating the operation time of the AMec system, we decided to make the application simply download the "nginx" image from the docker Hub, which size was 67.3 MB.

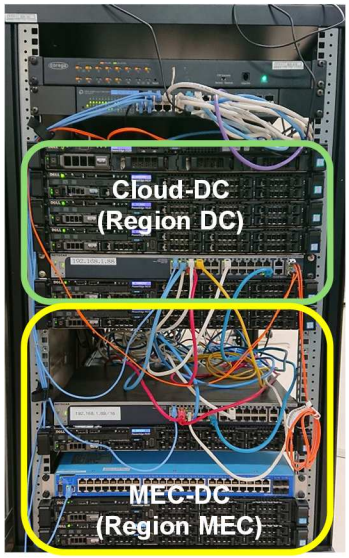

Fig.8 Cloud-DC and MEC-DC in the OpenLab.

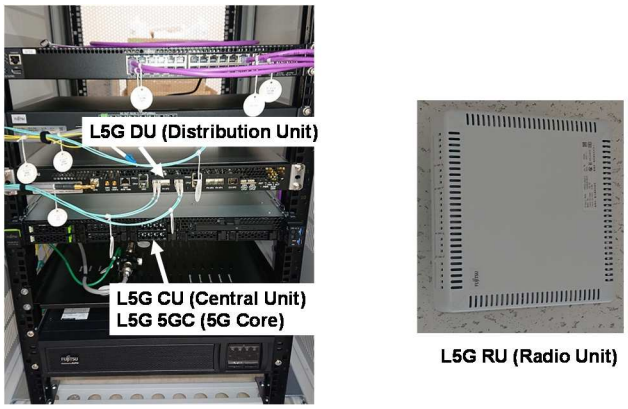

Fig. 9 Local 5G (L5G) system in the OpenLab.

The operation flow from receiving a request from the user to starting the application on AMec is as following. First, a user sends a request to the AMec controller via the frontend to start the application. Then, the AMec controller obtains information from the k8s-master through the k8s application programming interface (API), executes the allocation algorithm, and notifies the k8s-master of the results. The details of the scenario and the serial numbers of each step are as follows. These numbers correspond to the ones in Fig. 10. We measured the "user waiting time"' corresponds to from step #1 to #9 and its breakdown.

#0. The AMec controller and the frontend execute python files and standby as HTTP servers.
#1. User accesses to the frontend.
#2. The frontend forwards user's access to the AMec controller.
#3. The AMec controller obtains information on nodes and pods in the cluster via API from the k8s-master.
#4. The AMec controller executes the allocation algorithm and determines the pod allocation destination among k8s-workers shown in table 2.
#5. The AMec controller directs pod allocation to the k8s-master via API.
#6. The k8s-master configures each node to deploy pods.
#7. While each node pulls the image and the pod starts running, the AMec controller checks whether the pods and load balancing services are ready for the assigned application in 0.1 s via API to the k8s-master.
#8. When all assigned pods and services are ready, the AMec controller notifies to the user via the frontend that it is ready and the access port number for the frontend application.
#9. The frontend forwards the notification to the user.
#10. The user accesses to the frontend's port for the application.

Ten times experiments were conducted for each of the scenarios described above, with and without a container image cache on the node, and the user wait times and their breakdown were measured. The results are shown in Table 3. First, in the case with cache, user latency ranged from 4.42 s to 6.25 s, of which 94.3% to 96.5% were for #7. Without cache, user latency ranged from 11.86 s to 22.38 s, of which 98.1% to 98.9% were the time of #7. In particular, the average time to pull an image from the Docker Hub was 19.72 s for Raspberry Pi and 8 s to 9 s for the others. In without cache situation, the longest user waiting time was when a pod was assigned to the Raspberry Pi. Since the bandwidth was sufficient, we suspect that this is due to the read/write time of the SD card used for storage. Since it is necessary to wait until all pods and service in the application become ready, the waiting time becomes longer if even one of them is allocated to a low-performance node. Process #7 is the time spent waiting to pull and deploy the container image, which is the same time that occurs in a normal MEC environment. It was found that processes other than process #7, such as AMec-specific processes, account for less than 10 % of the user wait time. In particular, in the process #4, the allocation algorithm takes only 2 ms to 3 ms. The overhead of the AMec is very small.

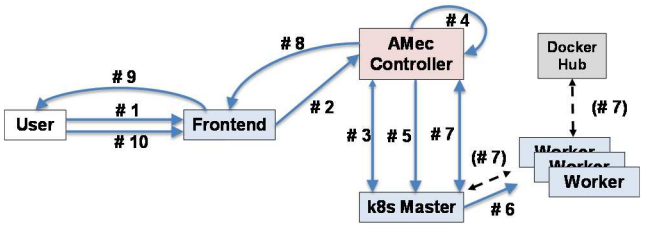

Fig.10 Experimental scenario of the AMec application.

We demonstrated that AMec can start services with user waiting times comparable to those of conventional MEC in the image cached case. Therefore, AMec, which utilizes surplus computing resources, can be considered a viable alternative to the conventional MEC.

TABLE III. USER WAITING TIME AND ITS BREAKDOWN

		#3	#4	#5	#7	Other	Total
Image Cached	Min	0.12 s (2.7%)	0.03 s (0.1%)	0.09 s (1.9%)	4.17 s (94.3%)	0.04 s (1.0%)	4.42 s
	Max	0.11 s (1.7%)	0.002 s (0.0%)	0.08 s (1.2%)	6.03 s (96.5%)	0.04 s (0.6%)	6.25 s
Image Not Cached	Min	0.11 s (0.9%)	0.003 s (0.0%)	0.07 s (0.6%)	11.63 s (98.1%)	0.04 s (0.4%)	11.86 s
	Max	0.11 s (0.5%)	0.003 s (0.0%)	0.08 s (0.4%)	22.13 s (98.9%)	0.05 s (0.2%)	23.38 s

B. *Feasibility Evaluation of Installed Hollow-Core Fiber Cables using Local 5G over PON System*

We have installed a 500 m length HCF cables in the OpenLab field at Spt. 2023. Fig. 11 shows the installed cable route. The cable has been installed across K, I, and O buildings in the Keio K2 campus. The installed cable is composed of two HCF cables and two SMF cables. Four fiber cables are terminated by LC connectors. To attach the LC connector to the HCF, few cm length SMF is spliced to the HCF. Therefore, we

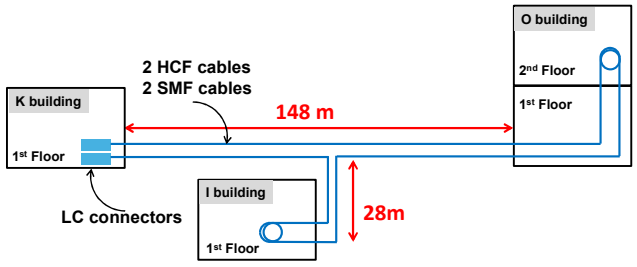

Fig.11 Installed 500 m HCF cable route in the Keio K2 campus.

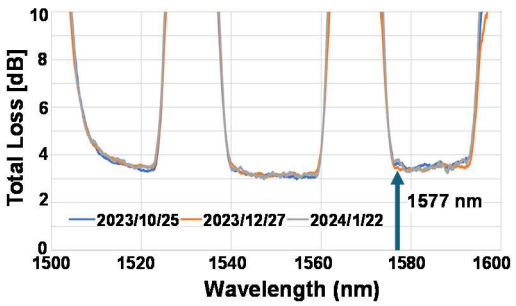

Fig.12 Installed 500 m HCF cable's loss spectrum in 4 months.

can easily connect a network equipment including the commercial 10G-EPON system to the installed HCF cable. The HCF cable loss penalty of the spliced SMF and LC connector is less than 1 dB. Fig. 12 shows a loss spectrum of the installed 500 m HCF cable. Measurements were taken in Oct., Dec. '23 and Jan. '24. Minimum 3 dB loss was observed involving LC connectors, and no damage was reported over 4 months.

Fig. 13 shows the experimental setup for evaluating applications on the terminals. Two Local 5G terminals (terminal #1 and #2) are housed in the L5G wireless access system. As shown in Fig. 9, the L5G system is composed of a 5G core network (5GC) system, a central unit (CU), a distribution unit (DU), and a radio unit (RU). Sub 6 (4.8 GHz) band is used in this L5G system. A mobile mid-haul (MMH) which is defied between CU and DU is accommodated into the 10G-EPON. This L5G system requires less than 1 ms latency and 9,578 bytes message transmission unit (MTU) size in the MMH section. The MMH is constructed by a layer 2 switch (L2 #1), an OLT, 15 km ODN, and an ONU. Less than 1 ms was achieved. Four Linux PC-based terminals are connected to the 10G-EPON system. Two PCs (terminal #3 and #4) are located at an OLT side and other two PCs (terminal #5 and #6) are located at an ONU side. The installed 500 m cable is inserted between the OLT and 1:4 optical splitter. In general, 10G-EPON systems use a simplex SMF cable for both OLT's and ONU's access network side ports. Both 1,577 nm wavelength signal for downlink and 1,270 nm wavelength signal for uplink are wavelength division multiplexed (WDM) into the simplex SMF cable. As shown in Fig. 12, the installed HCF cable can transmit the 1,577 nm signal. Unfortunately, the installed HCF cable cannot transmit the 1,270 nm signal. Therefore, we have installed two WDM filters for demultiplexing and multiplexing of both down and up-stream signals before and after the installed 500 m cable section. The downstream signal is transmitted in the HCF cable, and the upstream signal is transmitted in the SMF cable. After the installed cable section, an 1:4 splitter, an 1:8 splitter, 5 km and 10 km SMFs, and a 10 dB attenuator are set among tree ONUs (ONU#1 - #3) and OLT for constructing an ODN.

In this evaluation, two types of PON systems are constructed. They are a down/up-link asymmetric fiber PON (A-PON) system and a down/up-link symmetric fiber PON (S-PON) system. In the A-PON, the downlink uses the installed 500 m HCF cable, and the uplink uses the installed 500 m SMF cable. On the other hand, in the S-PON case, both down and up-links use the installed 500 m SMF cable for each. The installed HCF provides low latency and larger loss characteristics to the downlink of the 10G-EPON system. These characteristics can be observed at a PON manager. This is because an OLT measures a RTT on the order of nano-sec when an ONU is connected, and constantly monitors OLT's transmit optical signal power level and receiving optical signal power level from each ONU, and also receives power level information from the ONU side. Differences in latency and loss may affect the transmission characteristics of the 10G-EPON system, because current 10G-EPON standard does not mention the two fibers ODN application.

To evaluate the feasibility of the L5G MMH over A-PON, we evolved the PON system from simplex SMF PON to A-PON step by step. Fig. 14 shows the steps.

1st step - Duplex SMF PON: WDM is inserted between the OLT and the 1:4 splitter. 1 m SMFs are used.

2nd step - Emulated A-PON: 5 dB attenuator is inserted to the downlink and 1 km SMF is inserted to the uplink.

3rd step - S-PON: installed 500 m SMF cable is applied to both down/up-links.

4th step - A-PON: installed 500 m HCF cable is applied to the downlink.

We have successfully operate the L5G system in all steps. Measured distance and latency of ONU #1 at the PON manager is shown in Table 4.

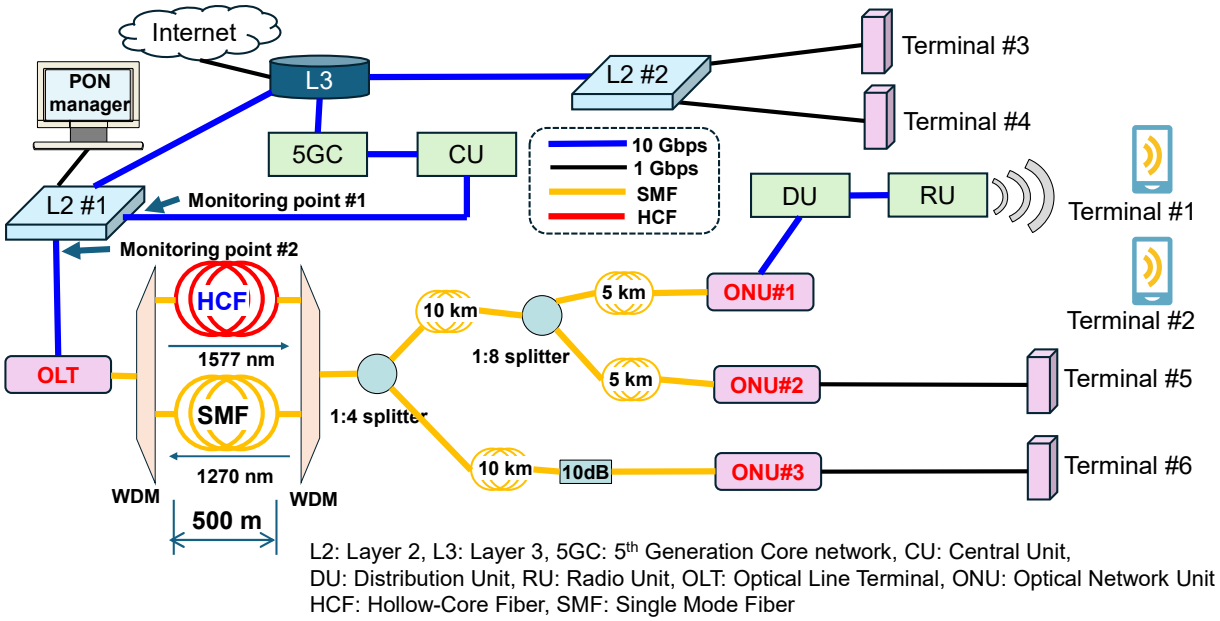

Fig.13 Experimental setup for evaluating application over 5G terminals and PCs. In the A-PON case, a down-stream signal of the PON is transmitted in the HCF. In the S-PON case, and SMF is used instead of the HCF.

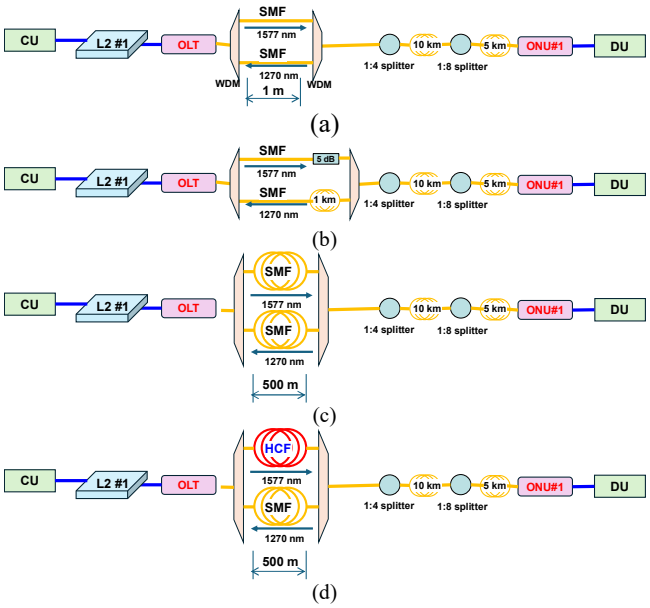

Fig.14 Evolution steps of the L5G MMH transmission. (a) Step 1: simplex to duplex. (b) Step 2: A-PON emulation. (c) Step 3: S-PON using installed SMF cables. (d) Step 4: A-PON using installed HCF cable and SMF cable.

TABLE IV. MEASURED DISTANCE AND LATENCY

Step	Distance (km)	Latency (μs)
1	15.254	74.744
2	15.753	77.192
3	15.845	77.640
4	15.763	77.240

Finally, we evaluated the feasibility of the installed HCF cables by measure the quality of applications. As an actual application which is run on terminals, a TCP/IP-based throughput measurement application "Microsoft NTttcp v5.39" [25] and file copy by Linux's "scp" are run between terminals. "NTttcp #1" is run from the L5G terminal #1 which is a Linux PC with L5G dongle as a sender side to the L5G terminal #2 which is also a Linux PC with L5G dongle as a receiver sider. "NTttcp #2" is run from the terminal #2 to the terminal #1. Both traffics are flowed from a sender terminal to a receiver terminal by loop back at the 5GC node. Upload throughput of the L5G system which is nearly 100 Mbps for one terminal restricts the maximum throughput of the application. "NTttcp #3" is run between the terminal #3 and the terminal #5. Traffic flow is from the terminal #5 => ONU#2 => OLT => L2#1 => layer 3 switch (L3) => L2#2, to the terminal #3, and vice versa. 1 Gbps is the

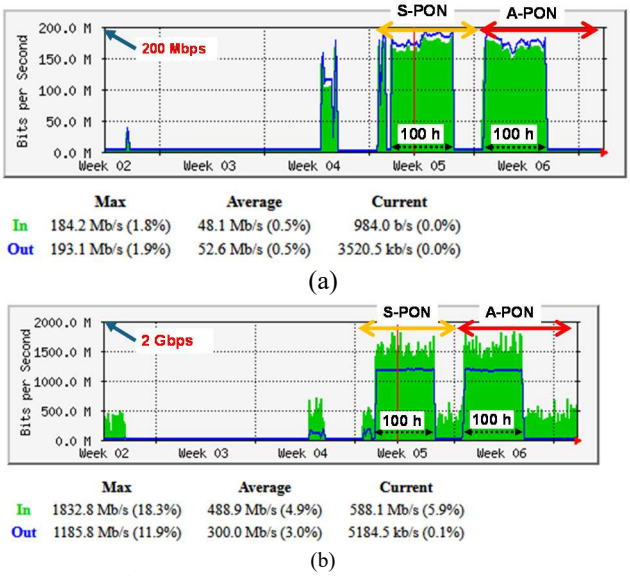

Fig.15 Throughput measurement results by MRTG. (a) at the monitoring point #1. (b) at the monitoring point #2.

maximum throughput which is restricted by the network interface card (NIC) of PCs. We also add a background traffic. Repeatedly copied a 50 GB file by "scp" is run between the terminal #4 and the terminal #6. "scp" can set used bandwidth limit as a command line option. Each file copy was performed in a randomly selected bandwidth from 100 Mbps to 1,000 Mbps in 100 Mbps increments. Traffic flow is from the terminal #6 => ONU#3 => OLT => L2#1 => L3 => L2#2, to the terminal #4, and vice versa. All four applications (3 "NTttcp" and 1 "scp") are run in parallel. Traffics are monitored at the L2#1 by using the Multi Router Traffic Grapher (MRTG) [26]. One way latency of each ONU is monitored at the PON manager. Optical power level of OLT and each ONU are also monitored at the PON manager.

We monitored L5G MMH traffic at the monitoring point #1 shown in Fig. 13 and all four applications' aggregated traffic at the monitoring point #2. Background "scp" application run during the entire experimental period. Three "NTttcp"s run in first 100 hour in the S-PON environment and next 100 hour in the A-PON environment. Fig. 15 shows the measured throughput at the monitoring point #1 in (a) and the monitoring point #2 in (b). No degradation is observed in the experiment from 5th to 6th week of 2024. This result shows the applied 10G-EPON can be run in the downlink uplink asymmetric latency environment and field installed HCF cables is stable.

TABLE V. LATENCY AND LINK LOSS MEASURED AT THE PON MANAGER

ONU#	Symmetric PON (SSMF)			Asymmetric PON (w/ HCF)			Differences		Remarks
	Distance (km)	*Latency (μs)*	*Link Loss (dB)*	*Distance (km)*	*Latency (μs)*	*Link Loss (dB)*	*Latency (μs)*	*Link Loss (dB)*	
#1	15.845	77.640	22.21	15.763	77.240	24.03	0.400	3.83	1 port ONU
#2	16.211	79.432	22.05	16.127	79.024	25.22	0.408	3.18	5 port ONU
#3	11.154	54.656	20.80	11.069	54.240	24.26	0.416	3.56	5 port ONU
Average							0.408	3.52	

We measured the 10G-EPON latency and link loss. The 10G-EPON latency is defined as RTT/2 between OLT and each ONU. The link loss is calculated from the sending power and received power of three ONUs. Measured results of the latency and the link loss of attached five ONUs are summarized in Table 5. The distance value is calculated from the latency value in the PON manger. As shown in the Table 1, theoretical latency differences of 500 m cable length between SMF and HCF is 0.78 µs. This should be led 0.39 µs (= 0.78 /2) difference in the A-PON latency case. Therefore, the measured average latency differences of 0.408 µs is good agreement. The measured average downlink loss penalty, i.e. HCF loss and connector splicing loss, was 3.52 dB.

IV. Conclusion

Two networking experiments in the Keio Future Photonic Network Open Laboratory were presented. The AMec PoC used the Local 5G access system, the MEC-DC, the cloud-DC, and JGN of the OpenLab. The feasibility of the AMec concept, which utilizes surplus computing resources of network equipment as workers in computing clusters was demonstrated. The real applications over the Local 5G access over 10G-EPON with field-installed 500 m PBGF-based HCF cables was successfully demonstrated and the feasibility of the installed HCF cables was confirmed by the throughput measurement of the actual applications.

Acknowledgment

The author is grateful to KEIO future photonic network Open Lab for providing experimental facilities. The author also appreciate for members in Keio Univ. , especially Mr. Koki Muramatsu for providing AMec experiment results and Prof. Naoaki Yamanaka for leading OpenLab, and members in Furukawa Electric and OFS for their technical supports and discussions.

References

[1] N. Yamanaka, M. Nishimura, M. Ishiguro, Y. Okazaki, T. Kawanishi, T. Tsuritani, A. Nakao, H. Harai, T. Hirooka, H. Furukawa, M. Miyazawa, N. Yamamoto, and S. Yoshino, “Beyond 5G era network vision - A bird’s-eye view of architecture and breakthrough technology towards 2030 -”, IEICE Tras. On Commun. B, Vol. J104-B No. 3, pp315-336, 2021 (written in Japanease).

[2] “Beyond 5G/6G white paper version 3.0,” NICT, 2023, Accessed: Mar. 25, 2024. [Online] Available: https://beyond5g.nict.go.jp/images/download/NICT_B5G6G_WhitePaperEN_v3_0.pdf .

[3] “Keio Future Optical Network Open Research Center homepage,” 2023, Accessed: Mar. 26, 2024. [Online] Available: https://pilab.jp/OpenLab/ .

[4] “OpNeAR Open Networking Advanced Research Lab,” UTD, 2001, Accessed: Mar. 26, 2024. [Online] Available: https://opnear.utdallas.edu/ .

[5] “IoT Networking Infrastructure Subcommiitee,” Research Promotion Council of Keihanna Info-Communication Open Laboratory, 2018, Accessed: Mar. 26, 2024. [Online] Available: https://www.khn-openlab.jp/bunkakai-gw/network/english.html .

[6] K. Mukasa, "Novel optical links using Hollow Core Fibers (HCFs)", IEICE Technical Report, PN2022-13, pp25-30, Aug. 2022 (written in Japanease).

[7] NICT, “JGN: High Speed R&D Network Testbed,” 2024, Accessed: Apr. 1, 2024. [Online] Available: https://testbed.nict.go.jp/jgn/english/index.html .

[8] P. J. Roberts, F. Couny, H. Sabert, B. J. Mangan, D. P. Williams, L. Farr, M. W. Mason, and A. Tomlinson, “Ultimate low loss of hollow-core photonic crystal fibres,” Opt. Express, 13, pp. 236-244, 2005, DOI: 10.1364/OPEX.13.000236

[9] J. M. Fini, J. W. Nicholson, R. S. Windeler, E. M. Monberg, L. Meng, B. Mangan, A. DeSantolo, and F. V. DiMarcello, "Low-loss hollow-core fibers with improved single-modedness," Opt. Express 21, pp. 6233-6242, 2013, DOI: 10.1364/OE.21.006233

[10] B. Zhu, B. J. Mangan, T. Kremp, G. S. Puc, V. Mikhailov, K. Dube, Y. Dulashko, M. Cortes, Y. liang, K. Marceau, B. Violette, D. Cartsounis, R. Lago, B. Savran, D. Inniss, and D. J. DiGiovanni, "First Demonstration of Hollow-Core-Fiber Cable for Low Latency Data Transmission," in 2020 Optical Fiber Communications Conference and Exhibition (OFC2020), San Diego, CA, USA, 2020.

[11] A. N. Kolyadin, A. F. Kosolapov, A. D. Pryamikov, A. S. Biriukov, V. G. Plotnichenko, and E. M. Dianov, "Light transmission in negative curvature hollow core fiber in extremely high material loss region," Opt. Express 21, pp. 9514-9519, 2013, DOI: 10.1364/OE.21.009514

[12] F. Poletti, "Nested antiresonant nodeless hollow core fiber," Opt. Express 22, pp. 23807-23828, 2014, DOI: 10.1364/OE.22.023807

[13] D. Richardson, "Hollow Core Fibers: Key Properties, Technology Status and Telecommunication Opportunities," in 2022 Optical Fiber Communications Conference and Exhibition (OFC2022), San Diego, CA, USA, 2022.

[14] Y. Hong, K. R. H. Bottrill, T. D. Bradley, H. Sakr, G. T. Jasion, K. Harrington, F. Poletti, P. Petropoulos, and D. J. Richardson, “Low-Latency WDM Intensity-Modulation and Direct-Detection Transmission Over >100 km Distances in a Hollow Core Fiber,” Laser & Photonics Reviews 2021, 15, 2100102, 2021, DOI: 10.1002/lpor.202100102

[15] V. Mikhailov, J. M. Fini, L. Meng, B. J. Mangan, J. W. Nicholson, R. S. Windeler, E. Monberg, F. DiMarcello, and P. S. Westbrook, "Low-loss low-latency transmission over single-mode hollow core fiber at 10 and 120 Gb/s," in 2014 Optical Fiber Communications Conference and Exhibition (OFC2014), San Francisco, CA, USA, 2014, DOI: 10.1364/OFC.2014.M2F.3.

[16] M. Kuschnerov, B. J. Mangan, J. Gong, V. A. J. M. Sleiffer, M. Herrmann, J. W. Nicholson, J. M. fini, L. Meng, R. S. Windeler, E. M. Monberg, A. DeSantolo, K. Mukasa, V. Mikhailov, U. Feiste, W. Zhang, and R. Yu, "Transmission of Commercial Low Latency Interfaces Over Hollow-Core Fiber," in Journal of Lightwave Technology, vol. 34, no. 2, pp. 314-320 2016, DOI: 10.1109/JLT.2015.2469144

[17] Z. Liu, B. Karanov, L. Galdino, J. R. Hayes, D. Lavery, K. Clark, K. Shi, D. J. Elson, B. C. Thomsen, M. N. Petrovich D. J. Richardson, F. Poletti, R. Slavik, and P. Bayvel, "Nonlinearity-Free Coherent Transmission in Hollow-Core Antiresonant Fiber," in Journal of Lightwave Technology, vol. 37, no. 3, pp. 909-916, 2019, DOI: 10.1109/JLT.2018.2883541

[18] S. Kimura, T. Takagi, K. Mukasa, and H. Tsuda, “+30.8 dBm, IM-DD, 32 Gbit/s High Power Optical Transmission with a 4-km Photonic Bandgap Fiber,” in 2023 International Conference on Photonics in Switching and Computing (PSC2023), Mantova, Italy, 2023, DOI: 10.1109/PSC57974.2023.10297221

[19] K. Murakami, S. Sugiura, H. Yamaji, M. Matsuura, T. Takagi, and K. Mukasa, “Over 1-Watt Analog RoF Signal Transmission Using a 1-km Hollow-Core Photonic Bandgap Fiber,” in 2024 Optical Fiber Communications Conference and Exhibition (OFC2024), San Diego, CA, USA, 2024.

[20] P. Gunning, “Bare-metal compute, storage and networking in metro optical access,” in 2019 24th OptoElectronics and Communications Conference (OECC) and 2019 International Conference on Photonics in Switching and Computing (PSC), WG1-4.A, Fukuoka, Japan, 2019, DOI: 10.23919/PS.2019.8818143

[21] S. Okamoto, K. Sugiura, M. Murakami, and N.Yamanaka, “Proposal of block-stream as a service-based access-metro edge computing technologies,” in 2020 IEICE Society Conference, B-12-2, Online, Sep 2020 (written in Japanese).

[22] K. Muramatsu, M. Murakami, Y. Uematsu, S. Okamoto, and N. Yamanaka, “Dynamic task assignment experiment for container-based in-network heterogeneous distributed mec environment,” in 19th IP/IoT & Processing + Optical Network (iPOP2023), T1-3, Tokyo, Japan, May 2023.

[23] K. Muramatsu, M. Murakami, Y. Uematsu, S. Okamoto, and N. Yamanaka, “Experiments of node’s automatic participation and collaboration with external services on amec (access-metro edge computing),” in International Conference on Emerging Technologies for Communications (ICETC2023), P1-13, Sapporo, Japan, 2023, DOI: 10.34385/proc.79.P1-13

[24] K. Muramatsu, Y. Uematsu, S. Okamoto, and N. Yamanaka, “Pod allocation algorithms to handle time-varying numbers of applications occurrence on the access-metro edge computing,” IEICE Communications Express, Vol. 13, Issue 2, pp. 35-38, 2024, DOI: 10.23919/comex.2023XBL0146

[25] GitHub, “Microsoft/ntttcp v5.39”, 2022, Accessed Apr. 8, 2024. [Online] Available: https://github.com/microsoft/ntttcp/ .

[26] Tobi Oetiker, “Tobi Oetiker’s MRTG – The Multi Router Traffic Grapher”, 2017, Accessed Apr. 8, 2024. [Online] Available: https://oss.oetiker.ch/mrtg/ .